Predesigned Covalent Organic Frameworks as Effective Platforms for Pd(II) Coordination Enabling Cross-Coupling Reactions under Sustainable Conditions

Alberto López-Magano, Rubén Mas-Ballesté, and José Alemán**

The phenanthroline unit in an imine-based covalent organic framework (Phen-COF) offers a robust coordination site for Pd(OAc)$_2$ centers. Coordination of palladium centers is demonstrated by a variety of techniques, including X-ray photoelectron spectroscopy and total X-ray fluorescence. The stable phenanthroline-Pd(II) coordination avoids leaching of metal centers to the reaction medium, where deactivation processes through nanoparticle formation limits the catalytic activities observed for homogeneous systems. Thus, because of isolation and immobilization of catalytic sites in the Pd@Phen-COF the performance of material, the catalytic outputs are dramatically increased with respect to the performance observed for analogous molecular catalysts. This concept is applied in this work to C—C cross-coupling reactions under mild and environmentally benign conditions. The activities found for Suzuki-Miyaura and Mizoroki-Heck reactions allow thousands of turnover numbers in the transformation of a wide scope of precursors with a high degree of recyclability. The results reported in this work contribute to the design of greener protocols for transformations that have a crucial role in the industrial synthesis of high-added value fine chemicals.

1. Introduction

Among the current synthetic tools in industrial scale, C—C bond formation through cross-coupling reactions is crucial for the synthesis of many compounds with interest in medicinal chemistry, polymers, materials, and fine chemicals,[1,2] Suzuki-Miyaura and Mizoroki-Heck reactions play a key role. In fact, they have become the preferred method of C—C bond formation, representing more than 30% of the total number of chemical transformations in the medicinal chemistry field.[3] Diverse metal-based catalytic systems have been designed since their discovery, involving the use of different sources of nickel, copper, cobalt, gold and, the most used, palladium.[4] However, the implementation of Pd-based catalytic systems is sometimes difficult due to the common inactivation of the catalyst, lixiviation of metal centers, and the subsequent contamination of the final products.[5] As a consequence of these drawbacks, the catalytic loadings of typical Mizoroki-Heck and Suzuki-Miyaura cross-couplings are relatively high, which implies an economical and environmental problem.[6] For all these reasons, the design of more and more reusable and stable Pd-based catalytic systems is increasingly in vogue.[1] One of the most powerful tools to achieve these goals consist of the use of heterogeneous catalysts,[7] such as zeolites,[8] metal organic frameworks (MOFs),[9] PEG derivatives,[10] conjugated microporous polymers (CMPs),[11] porous organic polymers (POPs),[12] and covalent organic framework (COFs).[13,14]

Among the heterogeneous catalysis strategies, covalent organic frameworks have become one of the most promising materials in a wide range of areas[13,14] such as artificial photosynthesis,[15] photocatalysis for organic synthesis,[16,17] photocatalytic degradation of pollutants,[18,19] metal catalysis,[20] and confined organocatalysis.[21] They are quite versatile, because of the possibility of tuning their structure, functionality, and pore size, depending on the designable building blocks of which they are composed of.[22] Following this line, COFs have been used as platforms for the incorporation of Pd centers following different strategies (**Figure 1**, left): predesign of pending arms in the constitutive building blocks (a), functionalization with Pd-NPs (b), and, the more explored, coordination to the iminic nitrogens of the COF backbone (c).[23]

First, the superficial functionalization of COFs and other related porous materials with highly active Pd(0) nanoparticles has been extensively explored.[24–26] However, coordination of single atom Pd(II) centers using COFs is a more challenging goal. One strategy to immobilize Pd(II) atoms consists of

A. López-Magano, R. Mas-Ballesté
Inorganic Chemistry Department
Módulo 7
Universidad Autónoma de Madrid
Madrid 28049, Spain
E-mail: ruben.mas@uam.es
R. Mas-Ballesté, J. Alemán
Institute for Advanced Research in Chemical Sciences (IAdChem)
Universidad Autónoma de Madrid
Madrid 28049, Spain
E-mail: jose.aleman@uam.es
J. Alemán
Organic Chemistry Department
Módulo 1
Universidad Autónoma de Madrid
Madrid 28049, Spain

The ORCID identification number(s) for the author(s) of this article can be found under https://doi.org/10.1002/adsu.202100409.

**ADVANCED
SCIENCE NEWS**
www.advancedsciencenews.com

**ADVANCED
SUSTAINABLE
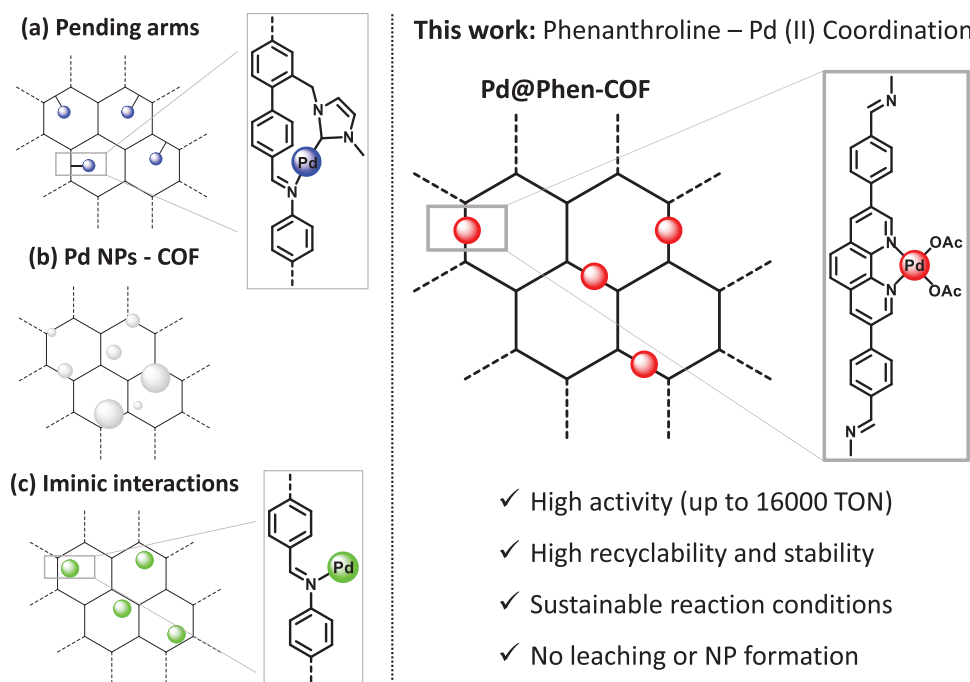SYSTEMS**
www.advsustainsys.com

Figure 1. Previous works regarding the functionalization of COFs with Pd (left), and strategy employed in this work (right).

introducing ligand fragments as pending arms. Following this idea, the introduction of N-heterocyclic carbenes as pending arms into the structure of an imine-based COF allowed a new platform to immobilize Pd(II) metal atoms.[27] From a more simple perspective, a pioneering work initially demonstrated the possible coordination of Pd(II) centers between the layers of an undecorated 2D-COF through iminic interactions.[28] This strategy was lately used in comparable imine-based materials, showing an interesting versatility, but restricted catalytic activities.[29–31] More recent studies also suggest that Pd atoms in a related material can be coordinated to amine structural defects of layered covalent organic frameworks.[32]

With all those precedents in hand, we can anticipate that the use of COF materials for these purposes would be significantly improved by using predesigned building blocks able to incorporate chelating ligands that stabilize the metal centers.[13] With this goal, we use in this work a phenanthroline-containing imine-based COF, which previously has been proved to stabilize metal centers such as Ni and Ir, allowing an unprecedented recyclability for dual photocatalytic systems.[33] Now, we extended the use of this material to Suzuki-Miyaura and Mizoroki-Heck cross-coupling reactions, with the aim to enhance the activity, recyclability, and stability of Pd centers, as a result of the strong interaction between the chelating phenanthroline ligand and metal atoms (Figure 1, right). Indeed, a coordination site that highly stabilize Pd(II) centers is required for achieving high recyclable catalytic systems, which could allow performing thousands of turnovers. However, typically Pd(II)-COFs systems are only able to perform few hundreds of TONs.[28–31] This is probably due to the low stability of Pd-COF iminic interactions (see the Supporting Information for a benchmarking catalytic activity). In this work, we addressed these challenges achieving up to 16 000 TONs under soft and environmentally friendly conditions, which is a milestone never reached with this kind of materials. The results shown below

demonstrate the high potential of this strategy, which allowed us to achieve excellent catalytic outputs. This system may permit the design of effective protocols using green solvents and avoiding metal contamination by achieving high conversions with low catalytic loadings.

2. Results and Discussion

2.1. Synthesis and Characterization

We performed the synthesis of the symmetric building block **1** through a double Suzuki cross-coupling between 3,8-dibromo-phenanthroline and the corresponding boronic acid derivative. Then, we proceeded to the synthesis of **Phen-COF** under the optimized solvothermal conditions (see optimization in the Supporting Information) by the combination of **1** and **TAPB** (**Scheme 1**), obtaining a layered bidimensional material.[33]

In order to functionalize the material with Pd(II), 20 mg of **Phen-COF** were dispersed in acetonitrile and aqueous acetic acid and treated with different quantities of Pd(OAc)$_2$ (1, 2.5, 5, and 11.5 mg, respectively) during 16 h at 70 °C (Table S1, Supporting Information). Interestingly, higher contents of Pd did not imply better catalytic activities (see below). The best result was obtained when 2.5 mg of Pd(OAc)$_2$ were incubated with 20 mg of **Phen-COF**, achieving 4.4% wt. of Pd (measured by total X-ray fluorescence [TXRF],[34] see Figure S2, Supporting Information). This value means that 26% of the phenanthroline moieties present in **Pd@Phen-COF** are coordinating Pd centers. The metal uptake from the solution has around 85% of effectivity in all the cases. This material was fully characterized with the same techniques than pristine **Phen-COF**, in order to demonstrate the retention and unalteration of the crystallinity, microstructure and chemical identity (**Figure 2**).

The powder X-ray diffraction pattern revealed the preservation and slight improvement of the crystallinity of the material after
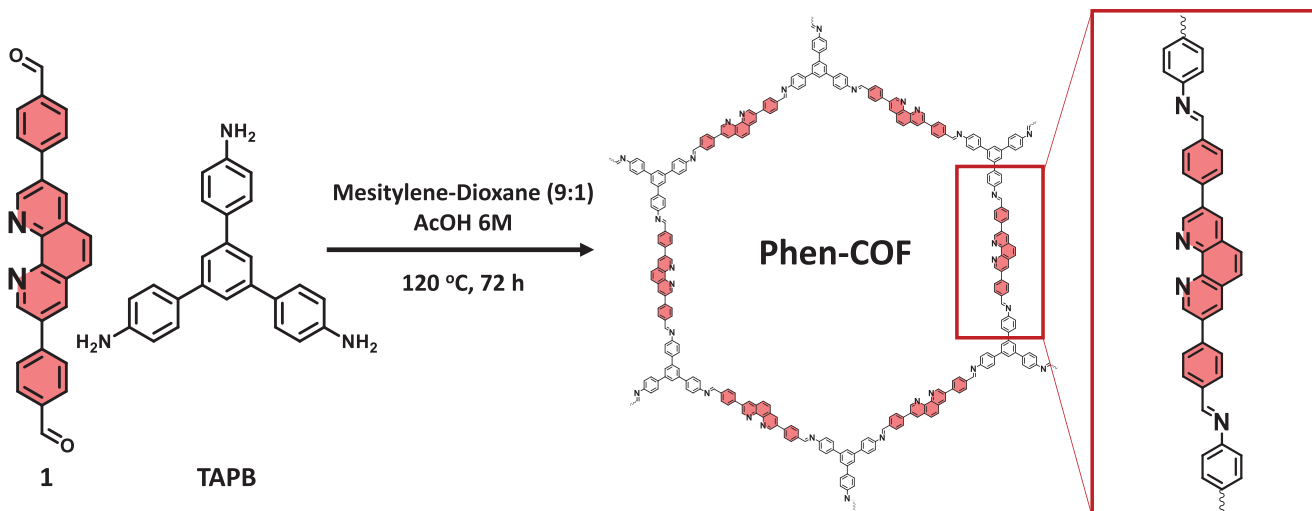
Scheme 1. Synthesis of **Phen-COF**.

post-functionalization treatment. Apart from the peak at $2\theta = 1.72°$, which corresponds to the (100) plane, two minor peaks at 2.98° and 3.44° are also distinguished (Figure 2a). Consistently, these two additional peaks of our experimental PXRD matched with the peaks corresponding to the (110) and (200) planes, respectively, in the eclipsed pattern simulated from the COF model.[33] Regarding N_2 adsorption/desorption isotherms, **Pd@Phen-COF** presents also moderated porosity. A slight decrease
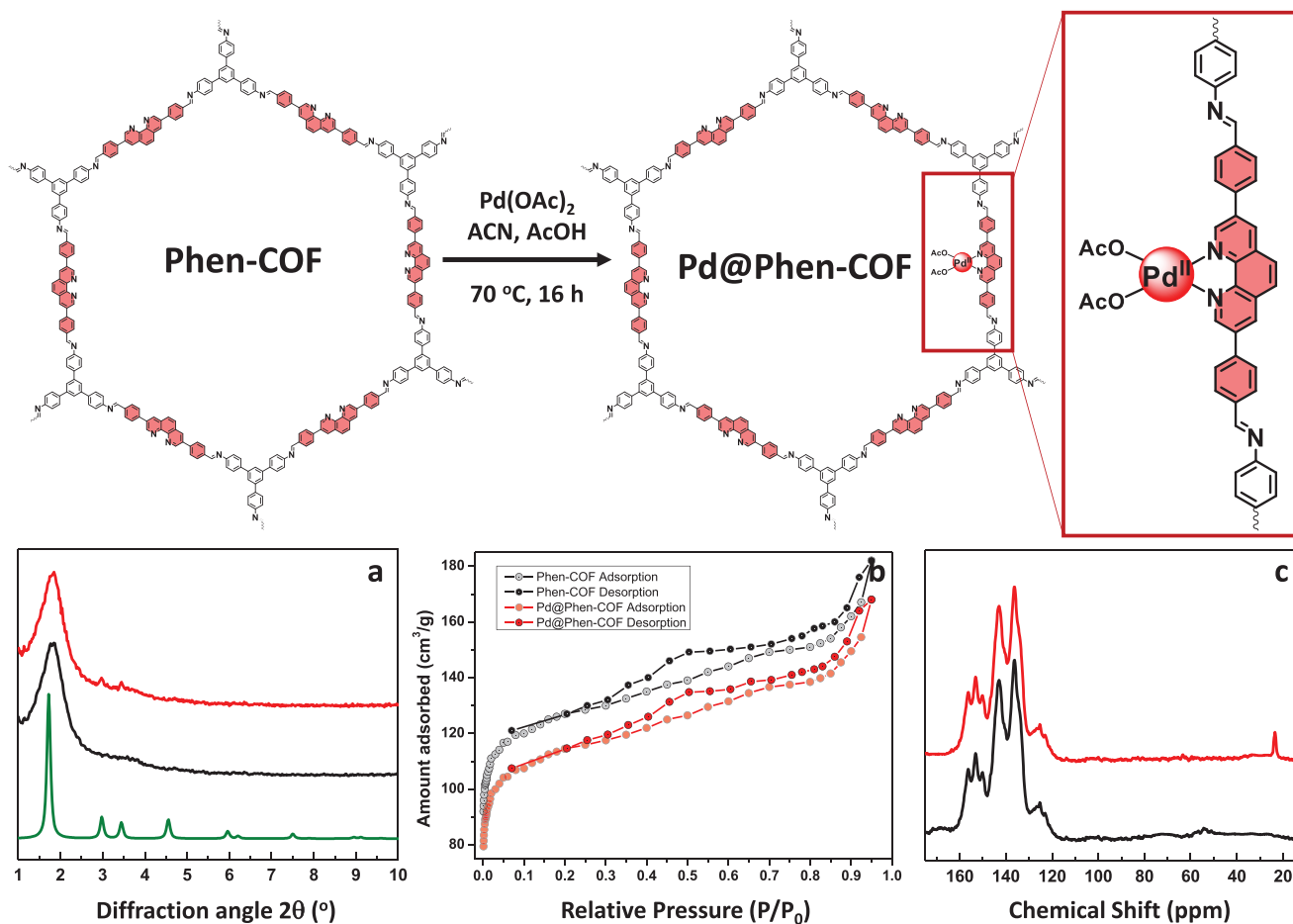

Figure 2. Synthesis and characterization of **Pd@Phen-COF**. The black lines correspond to pristine material, **Phen-COF**, while red lines correspond to **Pd@Phen-COF**. a) Experimental PXRD patterns compared to the theoretical one (green line). b) N_2 adsorption/desorption isotherms. c) ^{13}C CP/MAS NMR spectra.
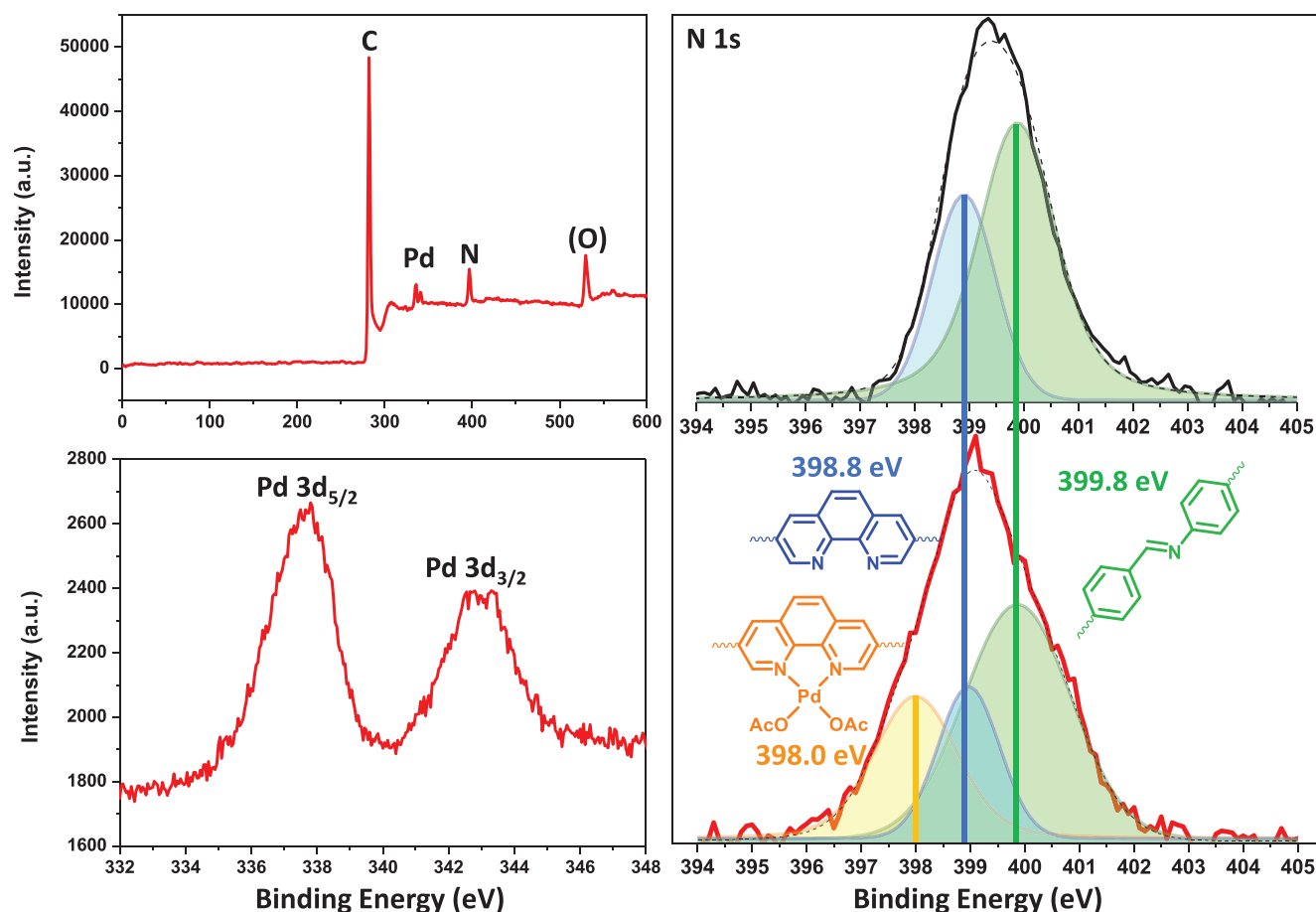
Figure 3. X-ray photoelectron spectroscopy measurements performed for **Pd@Phen-COF** (red line) and **Phen-COF** (black line).

in Brunauer–Emmett–Teller surface area (S_{BET}) in comparison with pristine Phen-COF was observed, from 482 to 447 m^2 g^{-1} (Figure 2b). This reduction was attributed to the coordination of Pd centers within the porous structure of the material.[35]

Solid-state cross-polarization magic angle spinning carbon-13 nuclear magnetic resonance (^{13}C CP/MAS NMR) spectrum of **Pd@Phen-COF** confirmed the preservation of the chemical structure of the material (Figure 2c). Only one minor additional peak was observed at 23 ppm, attributed to methyl group of acetate ligands present in the Pd coordination sphere.[28] The layered microstructure of the material was also preserved, as it can be seen from scanning electron microscopy images (Figure S3, Supporting Information).
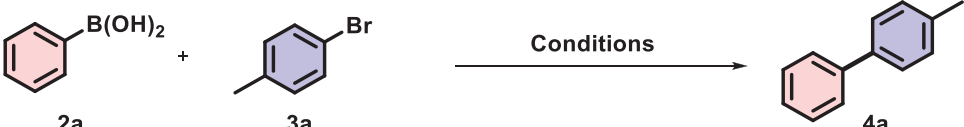
In order to prove the desired coordination of Pd into phenanthroline ligands, we performed X-ray photoelectron spectroscopy (XPS) measurements, where we found signals associated to C, N, and Pd atoms (**Figure 3**). The binding energies found for Pd $3d_{5/2}$ and $3d_{3/2}$ in **Pd@Phen-COF** were 337.8 and 342.8 eV, respectively. On the one hand, it is indicative of +2 oxidation state.[36] On the other hand, it is negatively shifted by 0.7 eV in comparison with Pd(OAc)$_2$ precursor.[37] This result is in accordance with XPS feature of model complex [Pd(phen)(OAc)$_2$],[28] suggesting the Pd coordination into phenanthroline fragments. N 1s XPS signature of the pristine COF can be described as the overlay of two peaks at 399.8 and

398.8 eV, which can be assigned to iminic and pyridinic nitrogens, respectively.[38] Interestingly, the presence of Pd centers has an impact on this signal. Thus, a fraction of nitrogen atoms that appear at 398.8 are shifted at 398.0 eV as a consequence of the coordination of Pd to phenanthroline ligands. However, the iminic signal at 399.8 eV remains unaltered, indicating that iminic nitrogen has a much lower tendency to interact with Pd atoms in this system. The energy-dispersive X-ray mapping images (SEM-EDX) showed the presence of homogeneously distributed C, N, and Pd atoms in the framework (Figure S5, Supporting Information), which is in accordance with XPS results.

2.2. Catalytic Application

The optimized content of Pd(II) in **Pd@Phen-COF** was determined by the study of catalytic performance for Suzuki-Miyaura-type cross-coupling between 4-tolylboronic acid and bromobenzene (**Table 1**). After 16 h of reaction at 80 °C, using a mixture EtOH-H$_2$O 4:1 as solvent and adding 6 equivalents of K$_2$CO$_3$ as base, moderate yields were observed. Interestingly, the better catalytic result was obtained with **Pd@Phen-COF** containing 4.4% wt. of Pd, but only reached 45% yield (Table 1, entry 2). Then, we proceeded to the optimization of the reaction with this material (see Table S2, Supporting Information),

**ADVANCED
SCIENCE NEWS**

www.advancedsciencenews.com

**ADVANCED
SUSTAINABLE
SYSTEMS**

www.advsustainsys.com

Table 1. Screening of conditions and control experiments for Suzuki-Miyaura cross-coupling.

Entry[a]	Catalyst	Solvent	Base	T [°C]	Conversion[b]
1	Pd@Phen-COF (1.9% Pd wt., 2.5 mg)	EtOH:H$_2$O 4:1 (2 mL)	K$_2$CO$_3$ (6 equiv.)	80	5
2	Pd@Phen-COF (4.4% Pd wt., 2.5 mg)	EtOH:H$_2$O 4:1 (2 mL)	K$_2$CO$_3$ (6 equiv.)	80	45
3	Pd@Phen-COF (8.3% Pd wt., 2.5 mg)	EtOH:H$_2$O 4:1 (2 mL)	K$_2$CO$_3$ (6 equiv.)	80	30
4	Pd@Phen-COF (15.0% Pd wt., 2.5 mg)	EtOH:H$_2$O 4:1 (2 mL)	K$_2$CO$_3$ (6 equiv.)	80	22
5	Pd@Phen-COF (4.4% Pd wt., 2.5 mg)	iPrOH:H$_2$O 4:1 (2 mL)	K$_2$CO$_3$ (1 equiv.)	25	>99
6	No catalyst	iPrOH:H$_2$O 4:1 (2 mL)	K$_2$CO$_3$ (1 equiv.)	25	0
7	Phen-COF	iPrOH:H$_2$O 4:1 (2 mL)	K$_2$CO$_3$ (1 equiv.)	25	0

[a]The reaction was carried out using 2a (0.15 mmol) and 3a (0.15 mmol) adding 2 mL of solvent and the corresponding base as additive. For more details on the optimization of the reaction, see Table S2 (Supporting Information); [b]Determined by ^{1}H-NMR.

observing full conversion and quantitative yield under soft and sustainable conditions (iPrOH-H$_2$O 4:1 as solvent, room temperature and only 1 equivalent of potassium carbonate as base, see Table 1, entry 5). In addition, no inert atmosphere was necessary, being possible to carry out the reaction under open-air conditions. The use of pristine **Phen-COF** without Pd(OAc)$_2$ or no catalyst only gave unfruitful results, indicating the need of the **Pd@Phen-COF** for the Suzuki reaction (Table 1, entries 6 and 7).

Under these optimized conditions, we decided to perform a comparative study with some homogeneous Pd complexes (Figure S6, Supporting Information). For example, the molecular analogues [Pd(phen)Cl$_2$] and [Pd(phen)(OAc)$_2$] were not able to produce any conversion, probably because of their insolubility. Moreover, typical Pd(OAc)$_2$, [Pd(PPh$_3$)$_4$] and [Pd(PPh$_3$)$_2$Cl$_2$] reached poor conversions in all the cases (never higher than 25%) at open-air conditions and r.t., observing the formation of a black powder after a catalytic run, which was attributed to the formation of agglomerated inactive Pd-PdO species.[39] Under less demanding conditions, these catalysts are typically used in C−C classical cross-couplings. However, the used conditions in this work, which are environmentally benign and soft, hamper their catalytic performance.

As full conversion was observed using **Pd@Phen-COF** (4.4% wt. Pd) as catalyst at 0.15 mmol reaction scale, we decided to evaluate the scalability and catalytic limit of our system by increasing the amount of reactants and solvent, but maintaining the content of material at 2.5 mg (Table S4, Supporting Information). Interestingly, full conversion was also observed at 0.30, 1.0, 2.0, 3.0, and 3.75 mmol scale (**Figure 4**), reaching a maximum TON of around 3500.

In order to evaluate the scope of the Suzuki-Miyaura reaction, the cross-coupling between different aryl bromides and aryl boronic acids using **Pd@Phen-COF** as catalyst was studied under the optimized conditions at 3.75 mmol scale,

approximately gram scale (**Figure 5**). Our system allowed the introduction of several electron-withdrawing and electron-donating groups in different positions of both aryl bromide and aryl boronic acid moieties (substrates **4a–4d**, **4g**, **41–4n**). Substrate **4e** represents an example of excellent selectivity of our system, instead of observing polymeric species or the activation of both bromides in 1,4-dibromobenzene, suggesting a confinement effect, which restricts the size of the final product. Moreover, the obtention of arylated heterocycles, such as substrate **4f**, or coupling of unprotected phenol **4h** showed the compatibility of our system with several functional groups. Finally, more hindered substrates such as **4n** and **4o** were also obtained in excellent yields. The TON observed in all the cases was around 3500.

A comparison between the catalytic behavior of homogeneous catalyst [Pd(PPh$_3$)$_4$] and material **Pd@Phen-COF** allowed us to determine the size selectivity as a result of the confinement of Pd centers. For this purpose, we designed a competitive reaction in which two different arylbromides with distinct steric hindrance
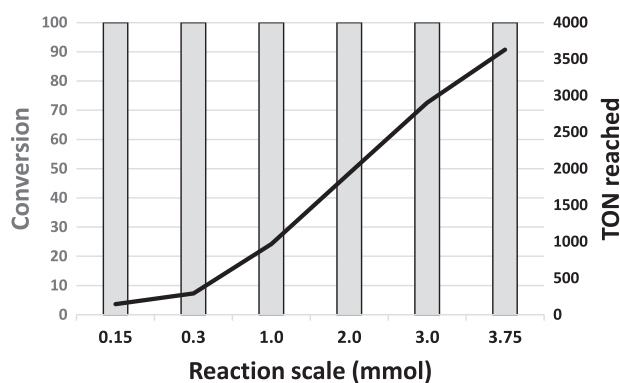

Figure 4. Study of the reaction scale for Suzuki-Miyaura cross-coupling using **Pd@Phen-COF** as catalyst.
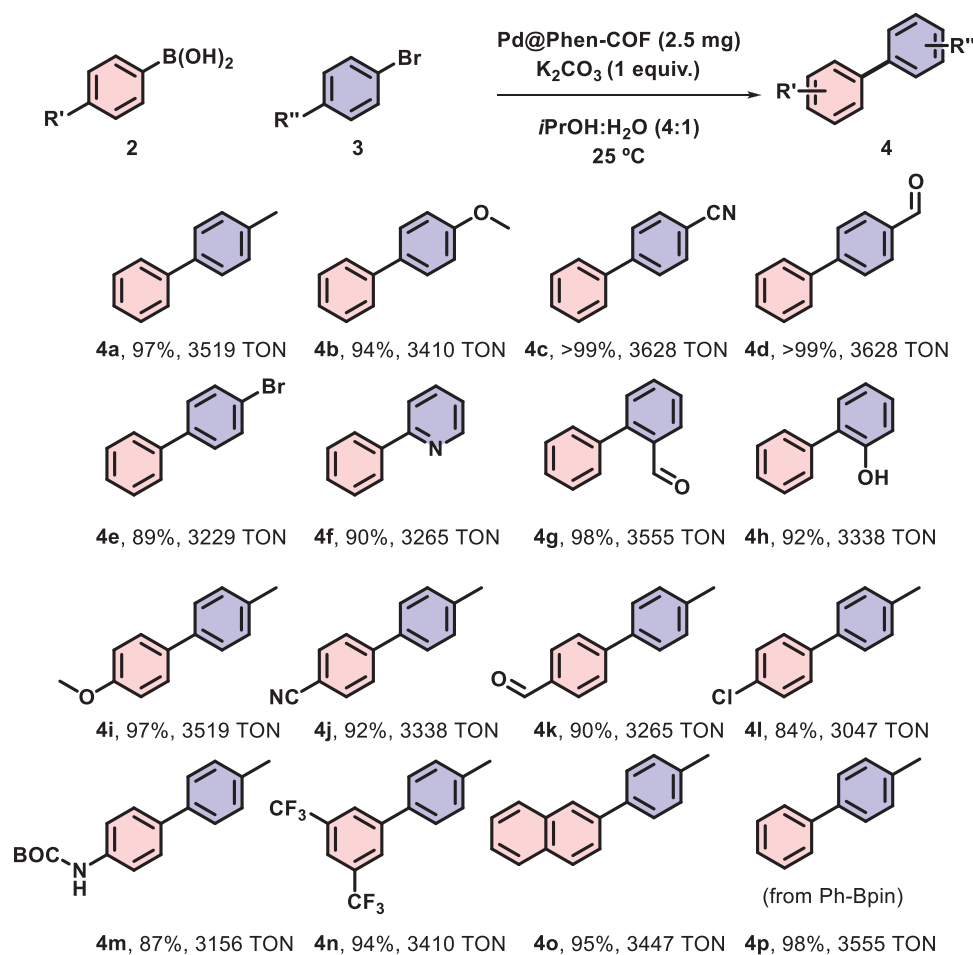
**ADVANCED
SCIENCE NEWS**

www.advancedsciencenews.com

**ADVANCED
SUSTAINABLE
SYSTEMS**

www.advsustainsys.com

Figure 5. Scope of Suzuki-Miyaura reaction. The reactions were carried out using **Pd@Phen-COF** (2.5 mg), 3.75 mmol of **2**, **3** and K₂CO₃ in 20 mL of *i*PrOH-H₂O (4:1) at room temperature during 16 h. The yields and TONs were calculated from the isolated product. For the characterization of the products, see Table S5 (Supporting Information).

were used. In particular, the homogeneously catalyzed reaction of *p*-tolyl boronic (**2i**) acid and a 1:1 mixture of 4-bromotoluene (**3i**) and 3,5-di-*tert*butylbromobenzene (**3j**) resulted on 70% conversion of the most hindered reagent, and only 30% conversion of 4-bromotoluene. In contrast, when using the material **Pd@Phen-COF**, this ratio was inverted, observing only 20%

conversion of the bulky substrate and 80% of the less hindered reagent **3i** (see the Supporting Information for details and **Scheme 2**). These observations strongly suggest that the cavity restraints act as molecular sieves, making less available the access of bulkier substrates. Thus, evidences for confined catalysis and the consequent size discrimination effect are found in this work.
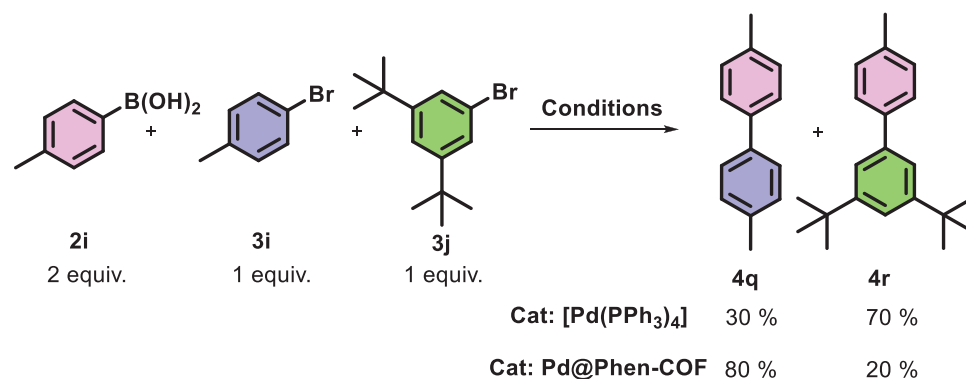
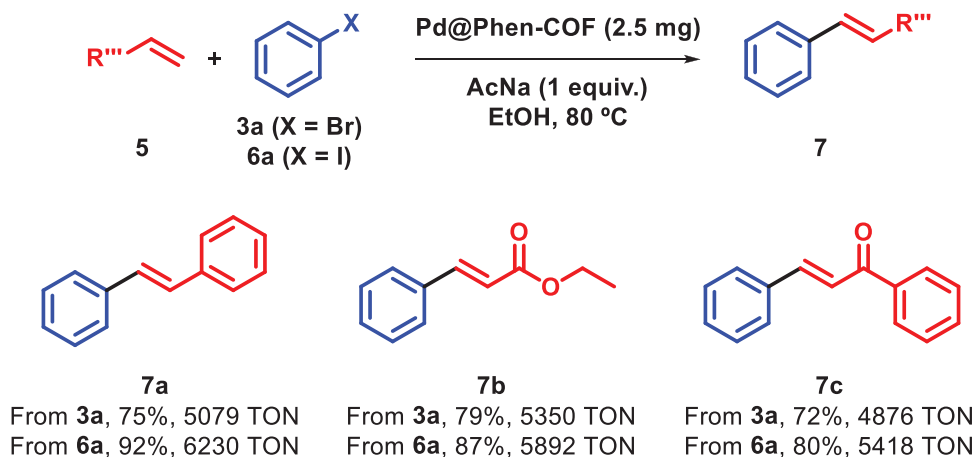**Scheme 2.** Size selectivity study under **Pd@Phen-COF** catalysis.

Figure 6. Scope of Mizoroki-Heck reaction. The reactions were carried out using **Pd@Phen-COF** (2.5 mg), 7.0 mmol of **5**, the corresponding halobenzene and sodium acetate in 20 mL of EtOH at 80 °C during 4 h. The yields and TONs were calculated from the isolated product. For the characterization of the products, see Table S5 (Supporting Information).

As another proof of the versatility of **Pd@Phen-COF**, we tested this material in Mizoroki-Heck cross-coupling reaction (**Figure 6**). After the optimization (see Tables S7 and S8, Supporting Information), the reaction between iodobenzene and styrene at 7 mmol scale took place in 92% yield in presence of 2.5 mg of **Pd@Phen-COF** after 4 h under refluxing ethanol and air atmosphere, using 1 equivalent of sodium acetate as a base. The use of other terminal olefins such as ethyl acrylate or methacrylophenone was also tolerated, giving excellent results in combination with both iodo- and bromo-benzene. The TONs reached variated from 4800 to 6200. Under these specific conditions, molecular $[Pd(phen)Cl_2]$, $[Pd(phen)(OAc)_2]$, $Pd(OAc)_2$, $[Pd(PPh_3)_4]$ and $[Pd(PPh_3)_2Cl_2]$ reached poor conversions (lower than 10%), producing a black-colored powder after 2 h of reaction.

2.3. Recyclability and Leaching Tests

A particularly interesting observation about the scope of this work is the simplicity of the isolation of the products, which only requires a filtration to eliminate the catalyst and subsequent extraction to separate the inorganic base from the pure product. Since full conversion was achieved in all the examples, and no byproducts were observed, no additional purification steps were necessary.

Owing the cost and high toxicity of Pd,[40] one important requirement of a designed catalytic system, especially for products intended for medicinal purposes, consists of avoiding contamination of the obtained final products by this metal. Molecular catalysts such as $[Pd(PPh_3)_4]$ or $Pd(OAc)_2$ commonly suffer deactivation processes, giving rise to the formation of nanoparticulated Pd/PdO species that are difficult to eliminate through simple procedures.[41] Thus, the design of robust and active heterogeneous functionalized materials that can immobilize Pd-active catalytic centers appears as an outstanding solution for this drawback.[42]

In our case, under the experimental conditions of the two proposed reactions, we have dismissed leaching processes and

contamination of the products by Pd in two different ways. First, the elimination of the catalyst after one catalytic run was performed by filtration. The subsequent filtrated solution was analyzed by inductively coupled plasma mass spectrometry (ICP-MS). The qualitative analysis of the supernatant revealed that no Pd atoms could be detected, discarding leaching processes. Moreover, the filtered solution was mixed with additional amounts of the starting materials, but no additional product was generated. Indeed, both essays confirmed that no Pd species were leached into the reaction media.

In addition, the recyclability and sturdiness of **Pd@Phen-COF** was confirmed in both studied reactions (**Figure 7**). In Suzuki-Miyaura reaction, this material was capable of performing, at least, five consecutive catalytic cycles with negligible loss of activity, generating 18 mmol of product **4a** using 5 mg of catalyst and achieving 8700 TON. In the case of Mizoroki-Heck reaction, **Pd@Phen-COF** generated 33 mmol (≈6 g with 5 mg of material) of product **7a** after five catalytic runs, attaining almost 16 000 TON. Indeed, these are the highest scale and TONs reached up to now regarding Suzuki-Miyaura and Mizoroki-Heck cross-couplings catalyzed by a Pd-functionalized COF (for comparison with other related works, see Table S11, Supporting Information).

The preservation of the chemical identity and structure of the catalytic material was confirmed by PXRD and FTIR. The stability of Pd centers was examined by XPS measurements, where the binding energy associated to Pd $3d_{5/2}$ was also found at 337.8 eV, confirming the +2 oxidation state and their remaining coordination to phenanthroline fragments.

3. Conclusion

The use of the phenanthroline containing imine-based covalent organic framework (**Phen-COF**) has been extended to the efficient coordination of Pd(II) centers. The available spectroscopic data demonstrate that phenanthroline is the preferential coordination site in the material framework. Although unfunctionalized COFs can also coordinate, to some extent, Pd(II) centers,
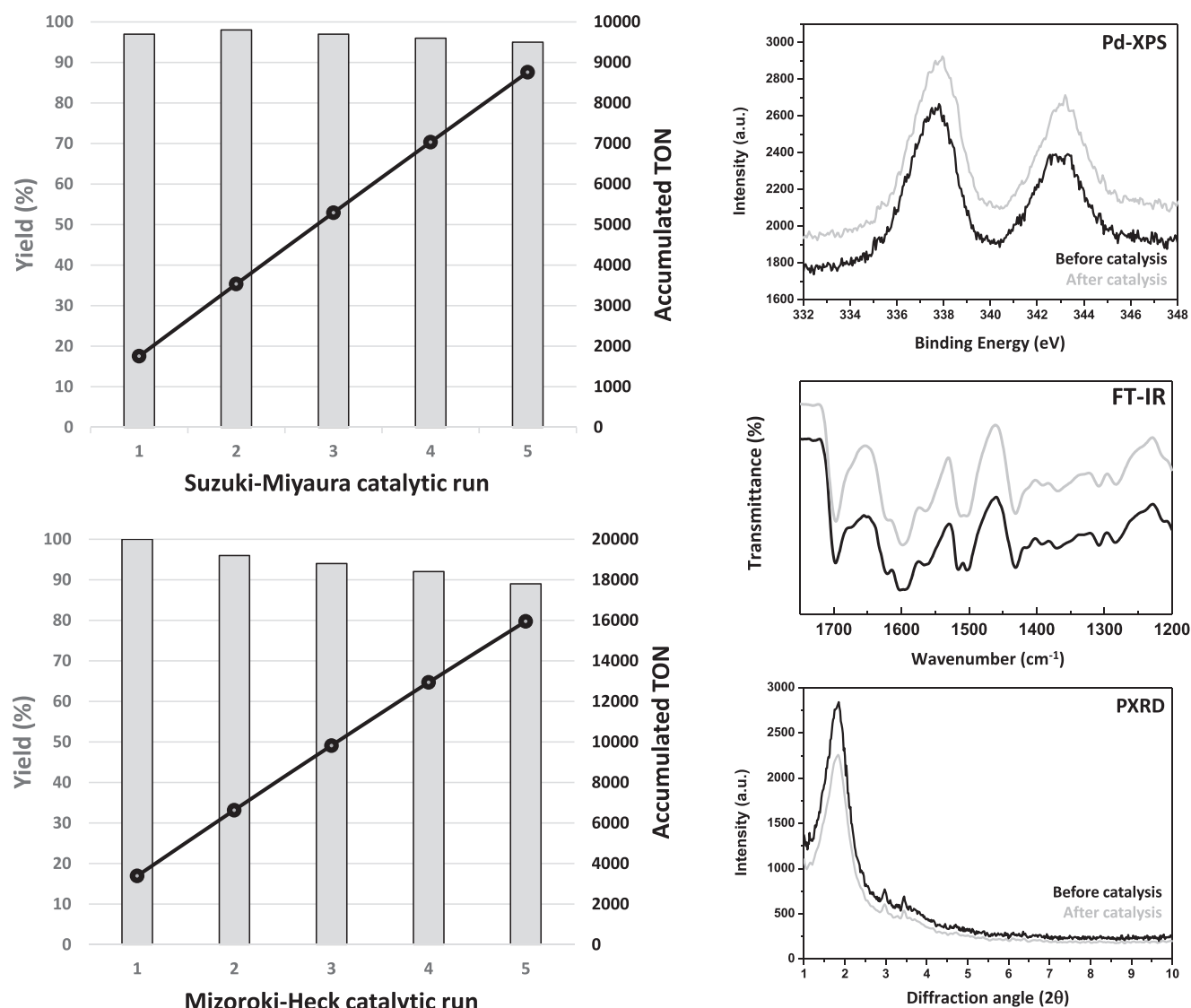
**ADVANCED
SCIENCE NEWS**

www.advancedsciencenews.com

**ADVANCED
SUSTAINABLE
SYSTEMS**

www.advsustainsys.com

Figure 7. Recyclability studies of **Pd@Phen-COF**. The stability of the material was checked by PXRD, FTIR, and XPS after a catalytic run (black colour before catalysis and grey colour after catalysis).

in these cases interactions between metal centers and the organic frameworks are not strong enough to prevent leaching of metallic fragments to the reaction media, which prevents high activities and recyclabilities. However, the material used in this work offers a robust alternative to immobilize catalytic $Pd(OAc)_2$ fragments, resulting on acute improvements of the catalytic performance when compared with analogous homogeneous systems or COFs that do not contain chelating sites such as phenanthroline. The versatility of the **Pd@Phen-COF** material is demonstrated for Suzuki-Miyaura and Mizoroki-Heck cross-coupling reactions, which are some of the most recurrent processes in the synthesis of fine chemicals. In fact, very high activities have been found for a wide range of substrates achieving values of TON up to 16 000. Interestingly, these reactions can be carried out under mild and environmentally benign conditions. Furthermore, the catalytic material can be recycled for several catalytic runs and leaching of molecular active species has been experimentally ruled out. Overall,

this work contributes to the use of catalytic metallized COFs specifically designed for the obtention of industrially relevant products, avoiding metal contamination and excess of reagents, and enabling the use of benign solvents and employment of green reaction conditions.

4. Experimental Section

Nuclear Magnetic Resonance: NMR spectra were acquired on a Bruker AV-300 spectrometer, running at 300 MHz for [1]H. Chemical shifts (δ) are reported in ppm relative to residual solvent signals ($CDCl_3$: 7.26 ppm for ^{1}H-NMR. [13]C solid state nuclear magnetic resonance was acquired on a Bruker AV-400 spectrometer coupled to a multinuclear probe ([15]N-^{31}P) CPMAS with triple channel (BL4 X/Y/^{1}H) for a 4 mm rotor at room temperature, using 1k scans and 12 kHz of turning speed. The ^{1}H excitation pulse used is $\pi/2 \times 2.75$ μs and the contact pulse is 3 ms.

Powder X-Ray Diffraction: PXRD patterns were obtained in a X'Pert PRO difractometer $\theta/2\theta$ geometry from Panalytical equipped with a Johansson monochromator for ʎ Kα, a X'Celerator fast detector in an

**ADVANCED
SCIENCE NEWS**

www.advancedsciencenews.com

**ADVANCED
SUSTAINABLE
SYSTEMS**

www.advsustainsys.com

alumina holder. The $\theta/2\theta$ swept was performed from 1° to 45° with an angular increase of 0.0167°/100 s.

Volumetric N_2 Sorption Isotherms: These were collected at 77 K (N_2) using an ASAP 2020 equipment from Micromeritics. Temperature was controlled by using a liquid nitrogen bath.

Scanning Electron Microscopy: SEM images were carried out on a Hitachi S-3000N electron microscope with a coupled ESED detector and an analyzer from energy dispersive X-ray from Oxford Instruments, INCAx-sight model. The images were obtained in vacuum after being metallized in a Sputter Quórum Q150T-S with gold coating.

Total X-Ray Fluorescence: TXRF analyses were performed with a benchtop S2 PicoFox TXRF spectrometer from Bruker Nano (Germany).[34,43] TXRF system was equipped with a Mo X-ray source working at 50 kV and 600 µA, a multilayer monochromator with 80% of reflectivity at 17.5 keV (Mo Kα), a XFlash SDD detector with an effective area of 30 mm², and an energy resolution better than 150 eV for 5.9 keV (Mn Kα). For deconvolution and integration commercial Spectra v. 7.5.3 software package from Bruker was used. Previously to the measurements, sample acid digestions were performed in a high pressure and temperature microwave. Acid digestion technology was used by means of an UltraWAVE digestion system from Millestone (Italy) with a single reaction chamber able to operate up to 199 bar pressure and 270 °C.

X-Ray Photoelectron Spectroscopy: XPS measurements were carried out using an electronic spectroscopic system SPECS GmbH equipped under ultra-high vacuum conditions (10^{-10} mbar), equipped with a PHOIBOS 150 9MCD energy analyzer, and a double anode X-ray source (Al/Mg). To compensate the surface charging of the samples, a source of electrons was used.

Synthesis of Pd@Phen-COF: in a 100 mL round-bottom flask, 140 mg of **Phen-COF** were suspended on 50 mL of dry acetonitrile and 1 mL of aqueous acetic acid 6 M during 30 min with an ultrasound bath. Then, Pd(OAc)$_2$ (17.5 mg, 0.078 mmol) was added. The mixture was stirred at 70 °C for 16 h, yielding an orange powder that was isolated by filtration and washed with THF. The resulting powder was washed with THF using Soxhlet extraction during 16 h, then filtered and dried first at room temperature under vacuum for 12 h, and then at 100 °C for 2 h to afford an orange powder.

General Procedure for Suzuki-Miyaura Cross-Coupling Catalyzed by Pd@Phen-COF: In a 50 mL round-bottom flask, 2.5 mg of Pd@Phen-COF (4.4% wt. Pd) were dispersed in 20 mL of a mixture iPrOH-H$_2$O 4:1 under an ultrasound bath. Then, the corresponding arylboronic acid 2 (3.75 mmol), aryl bromide 3 (3.75 mmol) and potassium carbonate (3.75 mmol) were added. The reaction mixture was stirred at 25 °C during 16 h. Then, the reaction was filtered, and extracted with 15 mL of dichloromethane and 15 mL of distilled water. The organic phase was dried over Na$_2$SO$_4$, filtered, and evaporated under reduced pressure. No further purifications were needed.

General Procedure for Mizoroki-Heck Cross-Coupling Catalyzed by Pd@Phen-COF: In a 50 mL round-bottom flask, 2.5 mg of Pd@Phen-COF (4.4% wt. Pd) were dispersed in 20 mL of EtOH under an ultrasound bath. Then, the corresponding olefin (7.0 mmol), aryl halide (7.0 mmol), and sodium acetate (7.0 mmol) were added. The reaction mixture was stirred at 80 °C equipped with a reflux condenser during 4 h. Then, the reaction was cooled down, filtered, and extracted with 15 mL of dichloromethane and 15 mL of distilled water. The organic phase was dried over Na$_2$SO$_4$, filtered, and evaporated under reduced pressure. No further purifications were needed.

Supporting Information

Supporting Information is available from the Wiley Online Library or from the author.

Acknowledgements

Conflict of Interest

The authors declare no conflict of interest.

Data Availability Statement

The data that support the findings of this study are available in the supplementary material of this article.

Keywords

[1] S. E. Hooshmand, B. Heidari, R. Sedghi, R. S. Varma, *Green Chem.* **2019**, *21*, 381.
[2] D. G. Brown, J. Boström, *J. Med. Chem.* **2016**, *59*, 4443.
[3] N. Miyaura, K. Yamada, A. Suzuki, *Tetrahedron Lett.* **1979**, *20*, 3437.
[4] L.-C. Campeau, N. Hazari, *Organometallics* **2019**, *38*, 3.
[5] C. E. Garrett, K. Prasad, *Adv. Synth. Catal.* **2004**, *346*, 889.
[6] J. Kielhorn, C. Melber, D. Keller, I. Mangelsdorf, *Int. J. Hyg. Environ. Health* **2002**, *205*, 417.
[7] P. P. Mpungose, Z. P. Vundla, G. E. M. Maguire, H. B. Friedrich, *Molecules* **2018**, *23*, 1676.
[8] A. Kumbhar, *Top. Curr. Chem.* **2016**, *375*, 2.
[9] A. Dhakshinamoorthy, A. M. Asiri, H. Garcia, *Chem. Soc. Rev.* **2015**, *44*, 1922.
[10] M. J. D. Pires, S. I. Purificação, A. S. Santos, M. M. B. Marques, *Synthesis* **2017**, *49*, 2337.
[11] Y. Song, P. C. Lan, K. Martin, S. Ma, *Nanoscale Adv.* **2021**, *3*, 4891.
[12] C.-A. Wang, K. Nie, G.-D. Song, Y.-W. Li, Y.-F. Han, *RSC Adv.* **2019**, *9*, 8239.
[13] J. L. Segura, S. Royuela, M. M. Ramos, *Chem. Soc. Rev.* **2019**, *48*, 3903.
[14] M. S. Lohse, T. Bein, *Adv. Funct. Mater.* **2018**, *28*, 1705553.
[15] H. L. Nguyen, A. Alzamly, *ACS Catal.* **2021**, *11*, 9809.
[16] A. López-Magano, A. Jiménez-Almarza, J. Alemán, R. Mas-Ballesté, *Catalysis* **2020**, *10*, 720.
[17] A. Jiménez-Almarza, A. López-Magano, L. Marzo, S. Cabrera, R. Mas-Ballesté, J. Alemán, *ChemCatChem* **2019**, *11*, 4916.
[18] A. Jiménez-Almarza, A. López-Magano, R. Cano, B. Ortín-Rubio, D. Díaz-García, S. Gomez-Ruiz, I. Imaz, D. Maspoch, R. Mas-Ballesté, J. Alemán, *Mater. Today Chem.* **2021**, *22*, 100548.
[19] J. Wang, S. Zhuang, *Coord. Chem. Rev.* **2019**, *400*, 213046.
[20] A. López-Magano, A. E. Platero-Prats, S. Cabrera, R. Mas-Ballesté, J. Alemán, *Appl. Catal., B* **2020**, *272*, 119027.
[21] J. Luis-Barrerra, R. Cano, G. Imani-Shakibaei, J. Heras-Domingo, J. Pérez-Carvajal, I. Imaz, D. Maspoch, X. Solans-Monfort, J. Alemán, R. Mas-Ballesté, *Catal. Sci. Technol.* **2019**, *9*, 6007.
[22] K. Geng, T. He, R. Liu, S. Dalapati, K. T. Tan, Z. Li, S. Tao, Y. Gong, Q. Jiang, D. Jiang, *Chem. Rev.* **2020**, *120*, 8814.

**ADVANCED
SCIENCE NEWS**

www.advancedsciencenews.com

**ADVANCED
SUSTAINABLE
SYSTEMS**

www.advsustainsys.com

[23] Z. Li, Y. Zhi, P. Shao, H. Xia, G. Li, X. Feng, X. Chen, Z. Shi, X. Liu, *Appl. Catal., B* **2019**, *245*, 334.

[24] D. Mullangi, S. Nandi, S. Shalini, S. Sreedhala, C. P. Vinod, R. Vaidhyanathan, *Sci. Rep.* **2015**, *5*, 10876.

[25] J.-C. Wang, C.-X. Liu, X. Kan, X.-W. Wu, J.-L. Kan, Y.-B. Dong, *Green Chem.* **2020**, *22*, 1150.

[26] M. Bhadra, H. S. Sasmal, A. Basu, S. P. Midya, S. Kandambeth, P. Pachfule, E. Balaraman, R. Banerjee, *ACS Appl. Mater. Interfaces* **2017**, *9*, 13785.

[27] J. Yang, Y. Wu, X. Wu, W. Liu, Y. Wang, J. Wang, *Green Chem.* **2019**, *21*, 5267.

[28] S.-Y. Ding, J. Gao, Q. Wang, Y. Zhang, W.-G. Song, C.-Y. Su, W. Wang, *J. Am. Chem. Soc.* **2011**, *133*, 19816.

[29] V. Sadhasivam, R. Balasaravanan, C. Chithiraikumar, A. Siva, *ChemistrySelect* **2017**, *2*, 1063.

[30] Y. Hou, X. Zhang, J. Sun, S. Lin, D. Qi, R. Hong, D. Li, X. Xiao, J. Jiang, *Microporous Mesoporous Mater.* **2015**, *214*, 108.

[31] R. S. B. Gonçalves, A. B. V. de Oliveira, H. C. Sindra, B. S. Archanjo, M. E. Mendoza, L. S. A. Carneiro, C. D. Buarque, P. M. Esteves, *ChemCatChem* **2016**, *8*, 743.

[32] I. Romero-Muñiz, A. Mavrandonakis, P. Albacete, A. Vega, V. Briois, F. Zamora, A. E. Platero-Prats, *Angew. Chem., Int. Ed.* **2020**, *59*, 13013.

[33] A. López-Magano, B. Ortín-Rubio, I. Imaz, D. Maspoch, J. Alemán, R. Mas-Ballesté, *ACS Catal.* **2021**, *11*, 12344.

[34] R. Fernández-Ruiz, A. von Bohlen, E. J. Friedrich K, M. J. Redrejo, *Spectrochim. Acta, Part B* **2018**, *145*, 99.

[35] P. van der Voort, H. Chen, W. Liu, A. Laemont, C. Krishnaraj, X. Feng, F. Rohman, Q. Zhang, M. Meledina, R. van Deun, K. Leus, *Angew. Chem., Int. Ed.* **2021**, *60*, 10820.

[36] A. C. Thomas, *Photoelectron and Auger Spectroscopy*, Plenum, New York **1975**.

[37] J. P. Mathew, M. Srinivasan, *Eur. Polym. J.* **1995**, *31*, 835.

[38] H. Lu, F. Ning, R. Jin, C. Teng, Y. Wang, K. Xi, D. Zhou, G. Xue, *ChemSusChem* **2020**, *13*, 3447.

[39] A. Biffis, P. Centomo, A. Del Zotto, M. Zecca, *Chem. Rev.* **2018**, *118*, 2249.

[40] T. Umemura, K. Sato, Y. Kusaka, H. Satoh, in *Handbook on the Toxicology of Metals* (Eds: G. F. Nordberg, B. A. Fowler), 4th ed., Academic, San Diego, CA **2015**, pp. 1113–1123.

[41] C. Amatore, A. Jutand, M. A. M'Barki, *Organometallics* **1992**, *11*, 3009.

[42] W. Yang, B. Vogler, Y. Lei, T. Wu, *Environ. Sci. Water Res. Technol.* **2017**, *3*, 1143.

[43] R. Fernández-Ruiz, M. J. Redrejo, E. J. Friedrich, M. Ramos, T. Fernández, *Anal. Chem.* **2014**, *86*, 7383.